Research Article

For reprint orders, please contact: reprints@futuremedicine.com

Nanomedicine

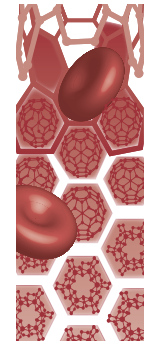

A computational framework for interspecies pharmacokinetics, exposure and toxicity assessment of gold nanoparticles

Aim: To develop a comprehensive computational framework to simulate tissue distribution of gold nanoparticles (AuNP) across several species. **Materials & methods:** This framework was built on physiologically based pharmacokinetic modeling, calibrated and evaluated with multiple independent datasets. **Results:** Rats and pigs seem to be more appropriate models than mice in animal-to-human extrapolation of AuNP pharmacokinetics and that the dose and age should be considered. Incorporation of *in vitro* and/or *in vivo* cellular uptake and toxicity data into the model improved toxicity assessment of AuNP. **Conclusion:** These results partially explain the current low translation rate of nanotechnology-based drug delivery systems from mice to humans. This simulation approach may be applied to other nanomaterials and provides guidance to design future translational studies.

First draft submitted: 12 August 2015; **Accepted for publication:** 24 September 2015; **Published online:** 11 November 2015

Keywords: biodistribution • computational nanotoxicology • endocytosis • nanomaterials • PBPK modeling • physiologically based pharmacokinetic modeling • phagocytosis • toxicokinetics

Zhoumeng Lin[1], Nancy A Monteiro-Riviere[2], Raghuraman Kannan[3] & Jim E Riviere*[,1]

[1]Institute of Computational Comparative Medicine (ICCM), Kansas State University, Manhattan, KS 66506, USA
[2]Nanotechnology Innovation Center of Kansas State (NICKS), Kansas State University, Manhattan, KS 66506, USA
[3]Department of Radiology, University of Missouri, Columbia, MO 65211, USA
*Author for correspondence:
Tel.: +1 785 532 3683
Fax: +1 785 532 4953
jriviere@ksu.edu

Numerous studies showed that exposure to some nanoparticles (NP) may be toxic to organisms [1-4]. Available *in vitro* and *in vivo* cellular uptake, pharmacokinetic and toxicity studies have different experimental designs that preclude comparing and combining results to gain deep insights into NP interspecies pharmacokinetics and risk assessment [5-8]. Therefore, it is crucial to have a meta-analysis method that can integrate available experimental and theoretical studies to systemically assess both NP pharmacokinetics and cellular toxicity across species, as well as to make *in vitro* to *in vivo* extrapolations (IVIVE) [8-12].

Compared with observational methods that are expensive and time-consuming, computational methods can offer a good adjunct to, or once validated, potentially substitute for predicting NP dosimetry and toxicity [12-15]. Both classical quantitative structure–activity/toxicity relationship (QSAR/QSTR) models [16,17] and advanced QSAR/QSTR perturbation models [18,19] have been successfully developed to predict cytotoxicity, ecotoxicity or antibacterial activity of many different NP under multiple experimental conditions (i.e., different cell types, exposure times, measurement methods, sizes, shapes and chemical compositions of NP). While QSAR/QSTR models are a useful *in silico* tool to predict toxic effects of chemicals or NP against diverse biosystems [16-19], they cannot be used to conduct interspecies extrapolation or IVIVE of target tissue dosimetry and toxicity.

Physiologically based pharmacokinetic (PBPK) modeling is one computational approach that simulates the absorption, distribution, metabolism and elimination (ADME) of chemicals and/or NP in the body using mathematical equations. Well-

Future Medicine part of fsg

validated PBPK models may be used to conduct IVIVE and interspecies extrapolation of NP tissue dosimetry and toxicity [11,12]. Many investigators have tried to develop PBPK models for NP in rodents [20-23], but none of the available models are comprehensive enough to conduct IVIVE and interspecies extrapolation.

Recently, we have developed a PBPK model for gold nanoparticles (AuNP) in mice [23]. AuNP were selected as model NP because they are used widely in nanomedicine [24] and there are sufficient pharmacokinetic and toxicity data for developing a well-validated model [2,5,23]. Based upon this mouse model [23], the objective of this study was to create a comprehensive computational framework that could simulate the tissue distribution of AuNP across several species, as well as incorporate *in vitro* and *in vivo* cellular uptake and toxicity data to inform pharmacokinetics, exposure and toxicity assessment. Therefore, we optimized and extended the mouse model to simulate the kinetics of AuNP in rats and pigs. The rat and pig models were evaluated with independent datasets to ensure the validity of the model. Then, the rodent and porcine models from various exposure scenarios were independently scaled to humans to determine the optimum model for animal-to-human extrapolation of NP pharmacokinetics (Figure 1). The derived optimal human model was then used as a framework for incorporating *in vitro* and *in vivo* toxicity data to predict the associated human equivalent doses for risk assessment.

Materials & methods

Data source & model structure

The data for rat and pig PBPK model calibration were obtained from the published literature [25-27]. As detailed in Supplementary Table 1, this model is primarily for AuNP coated with polyethylene glycol (PEG), gum arabic or citrate, and only pharmacokinetic data for these types of AuNP with at least four measurement time points were selected for model calibration. The model structure was based on our mouse PBPK model with minor modifications [23]. Briefly, it consisted of seven compartments: plasma (or blood), liver, spleen, kidneys, lungs, brain and rest of body (Figure 1). The same methods [23] describing transcapillary membrane transport with a membrane-limited approach, uneven distribution between plasma and tissue using the term 'distribution coefficient' and endocytosis with the Hill function, as well as biliary and urinary excretion using a first-order equation were applied in the present model. Dissolution of AuNP was not considered due to lack of experimental evidence [5]. To simplify the model and increase its harmonization, a general approach describing endocytosis of AuNP from blood to tissue phagocytic cells was used across all species (Figure 1). In order to simulate dose dependency, the term maximum uptake capacity for each tissue (except the brain) was included. AcslX version 3.0.2.1 (Aegis Technologies Group, Inc., AL, USA) was used to run all simulations. Model code in continuous simulation language (CSL) format is provided in the Supplementary Information as well as our website [28].

Model parameterization

Physiological parameters for mice, rats, pigs and humans are provided in Supplementary Table 2 [25,26,29-35]. NP-specific parameters used in the mouse PBPK model [23], such as distribution coefficients and permeability coefficients, were kept the same in the present model. This creates the most parsimonious model by using a minimum number of estimated parameters and applying a generic value for parameters across species. Endocytic parameters for each type of AuNP (application size domain: 13–100 nm) in each species had to be re-estimated by using the same approach used in the mouse model [23] because uptake of NP depends on the size, dose, surface coating, cell type and species [6]. The urine elimination rate in the pig model was estimated by visually fitting to the urine data in the pig study [25]; this optimized parameter value was used in the rat and human models. All NP-specific parameters are provided in Supplementary Table 3.

Model evaluation

The overall goodness of fit between simulated and experimental data was evaluated with linear regression analysis using GraphPad Prism 6 (GraphPad Software Inc., CA, USA). The predictive ability of the rat and pig models was evaluated with other studies where similar types and doses of AuNP were used (Supplementary Table 1) [36,37]. The criterion of a validated model was based on WHO guidelines, namely, a model is considered reasonable if simulation results are within a factor of two of independent experimental data [38]. Sensitivity and uncertainty analyses have been conducted and reported in the mouse model [23] and, therefore, were not repeated in this study.

Model cross-species extrapolation

Model extrapolation from mice, rats and pigs to humans was conducted by changing physiological parameters to be human-specific and keeping NP-specific parameters the same as in the original animal models. The derived human models were then used to predict the blood kinetics of a nanomedicine CYT-6091, a rhTNF-bound PEG-coated 27-nm AuNP, after intravenous (iv.) injection in advanced-

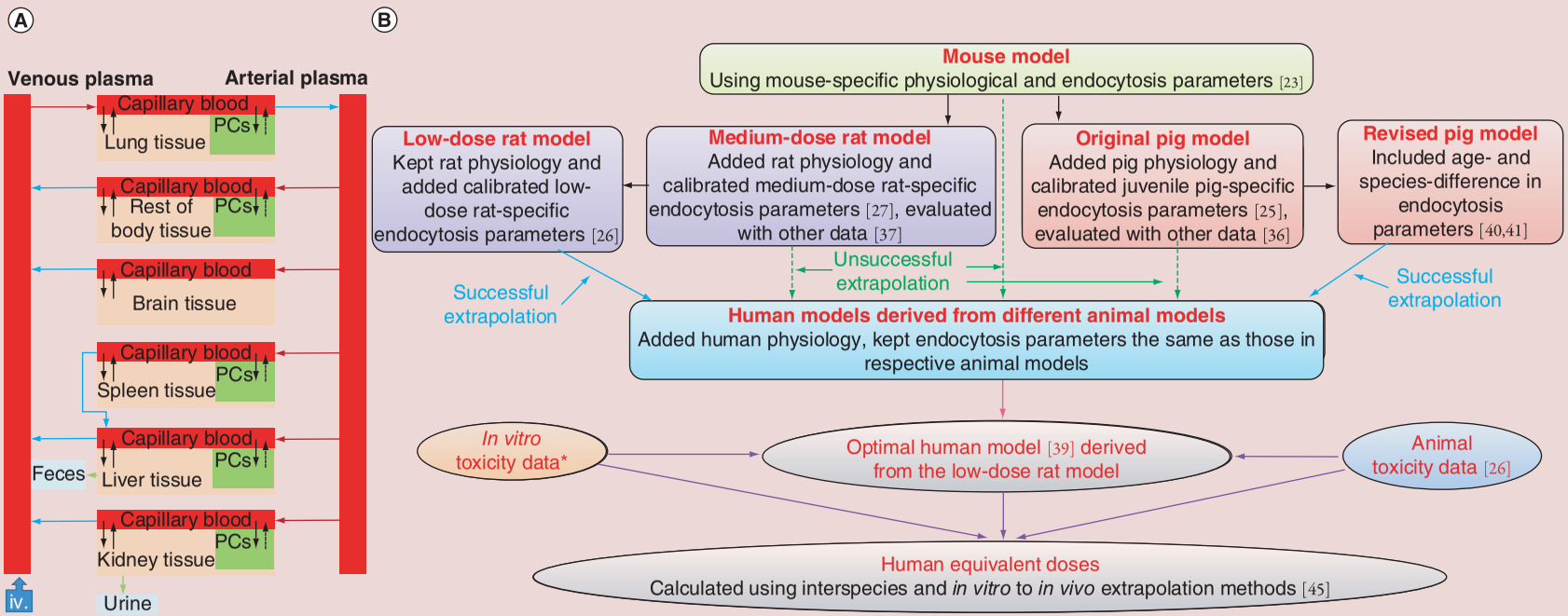

Figure 1. Schematic representation of the study design. (A) (left side): Schematic diagram of the physiologically based pharmacokinetic model for gold nanoparticles in mice, rats, pigs and humans. PCs is our operational term for various phagocytic cells, including reticuloendothelial system and organ-specific cells, such as liver Kupffer cells, splenic macrophages, kidney mesangial cells etc. **(B)** (right side): Flowchart of the physiologically based pharmacokinetic model development, evaluation, dose extrapolation, species extrapolation and *in vitro* to *in vivo* extrapolation processes. Black arrows represent animal-to-animal extrapolation by using animal-, dose- and age-specific physiological and endocytic parameters. Green dashed and blue solid lines represent animal-to-human extrapolation by using human-specific physiological parameters; endocytic parameters were kept the same as those in respective animal models. Green dashed lines indicate unsuccessful extrapolation, while blue solid lines indicate successful extrapolation. Purple lines represent rat-to-human extrapolation and *in vitro* to *in vivo* extrapolation of toxicity data of gold nanoparticles. Reference citations are given in square brackets.
*References listed in Supplementary Table 4.
iv.: Intravenous.

stage cancer patients [39]. Besides direct model extrapolation from laboratory animals to humans, a revised approach based on the relative density of phagocytic cells in the liver of juvenile pigs compared with adult humans was tested. Briefly, based on the evidence that the density of Kupffer cells in juvenile pigs is around sevenfold (0.89×10^6 vs 0.13×10^6 cells/g liver tissue) higher than in adult humans [40,41], in addition to changing physiological parameters to be human-specific, the juvenile pig model was scaled to humans by decreasing the maximum endocytic rates and capacities by sevenfold. Simulations using human models derived from different approaches (mouse model, medium-dose rat model, low-dose rat model, original pig model and revised pig model) were compared with experimental data [39] to determine the optimal human model.

Model application

To show model application in exposure and risk assessment, the optimal human model was used to predict blood and liver Au concentrations after iv. injection with AuNP across a wide dose range (0.001–100 mg/kg). This dose range was selected based on the doses used in the laboratory animals [2,5]. The liver was selected as the target organ because AuNP predominantly accumulate in the liver after exposure regardless of exposure route, dose, size and species [5,42]. To assess the risk of AuNP exposure, a literature review on the *in vitro* and *in vivo* toxicity of AuNP was carried out and representative results are provided in Supplementary Table 4. Next, the human equivalent doses associated with representative *in vitro* cytotoxic concentrations of AuNP in primary human tissue [43] and blood cells [44], as well as the reported *in vivo* toxic dose in rats [26], were predicted by using the human PBPK model based on the IVIVE and species extrapolation methods [45]. Specifically, the human equivalent doses were the doses when simulated maximum liver Au concentrations were equal to the reported *in vitro* cytotoxic nominal concentrations or the doses resulting in identical maximum liver Au concentrations in rats where adverse effects were observed.

Results

Model development in rats & pigs

Our mouse PBPK model [23] was scaled to rats and pigs (Figure 1) by using species-specific physiological and endocytic parameters (Supplementary Tables 2 & 3). Model simulation results were well correlated to the observed concentrations or amounts of Au in the blood, liver, spleen, kidneys, lungs and/or urine of rats [27] and pigs [25] after iv. exposure to 0.8 and 2.0 mg/kg AuNP, respectively (Figure 2). The determination coefficients (R^2) between simulated and measured data were 0.98 for both models. These results suggest that the rat and pig PBPK models at doses from 0.8 to 2.0 mg/kg have been calibrated properly.

Evaluation of the rat & pig models

The predictive capability of the rat and pig models was then evaluated with independent datasets [36,37] (Supplementary Table 1). Both models adequately simulated the observed liver and spleen concentrations of Au, differing less than twofold (Supplementary Figure 1), which is considered 'validated' according to the WHO PBPK model evaluation criterion [38]. These results suggest that both the rat and pig models have excellent predictive capability of the tissue distribution of AuNP.

Model extrapolation from medium to low doses

Since the doses used in the animal studies were generally higher than the actual doses that humans are exposed to and NP pharmacokinetics is dose dependent, it is critical to have a low-dose model [5,39]. Therefore, the rat model for medium doses (~1.0 and ~0.01 mg/kg were defined as medium and low doses, respectively) was extrapolated to simulate low-dose kinetics of AuNP [26] using low-dose-specific endocytic parameters (Supplementary Table 3). Simulation results matched the observed Au concentrations [26] in blood, liver, spleen, kidneys and lungs of rats after low-dose iv. administration ($R^2 = 0.98$; Supplementary Figure 2), suggesting that the low-dose model was calibrated properly.

Model application: predictions of dose-dependent tissue distribution

To reveal NP dose-dependent kinetics, we employed the medium-dose and low-dose rat models to predict percentage tissue distribution of the injected dose (%ID). The results showed that both absolute (%ID) and relative (%ID/g tissue) distributions primarily to phagocytic organs (e.g., liver, spleen and lungs) were consistently several fold higher in the medium-dose than in the low-dose groups (Figure 3). Next, we compared the simulated endocytic rates in liver and spleen of rats after iv. injection with the same dose of AuNP (0.01 mg/kg) using both the models. We noticed that the low-dose model-predicted liver and spleen endocytic rates were approximately four- to fivefold lower than the predicted rates by the medium-dose model (Supplementary Figure 3). These data suggest that, besides surface coatings and sizes [6], endocytosis of AuNP is highly dependent on the dose and it may be a key contributing factor to their

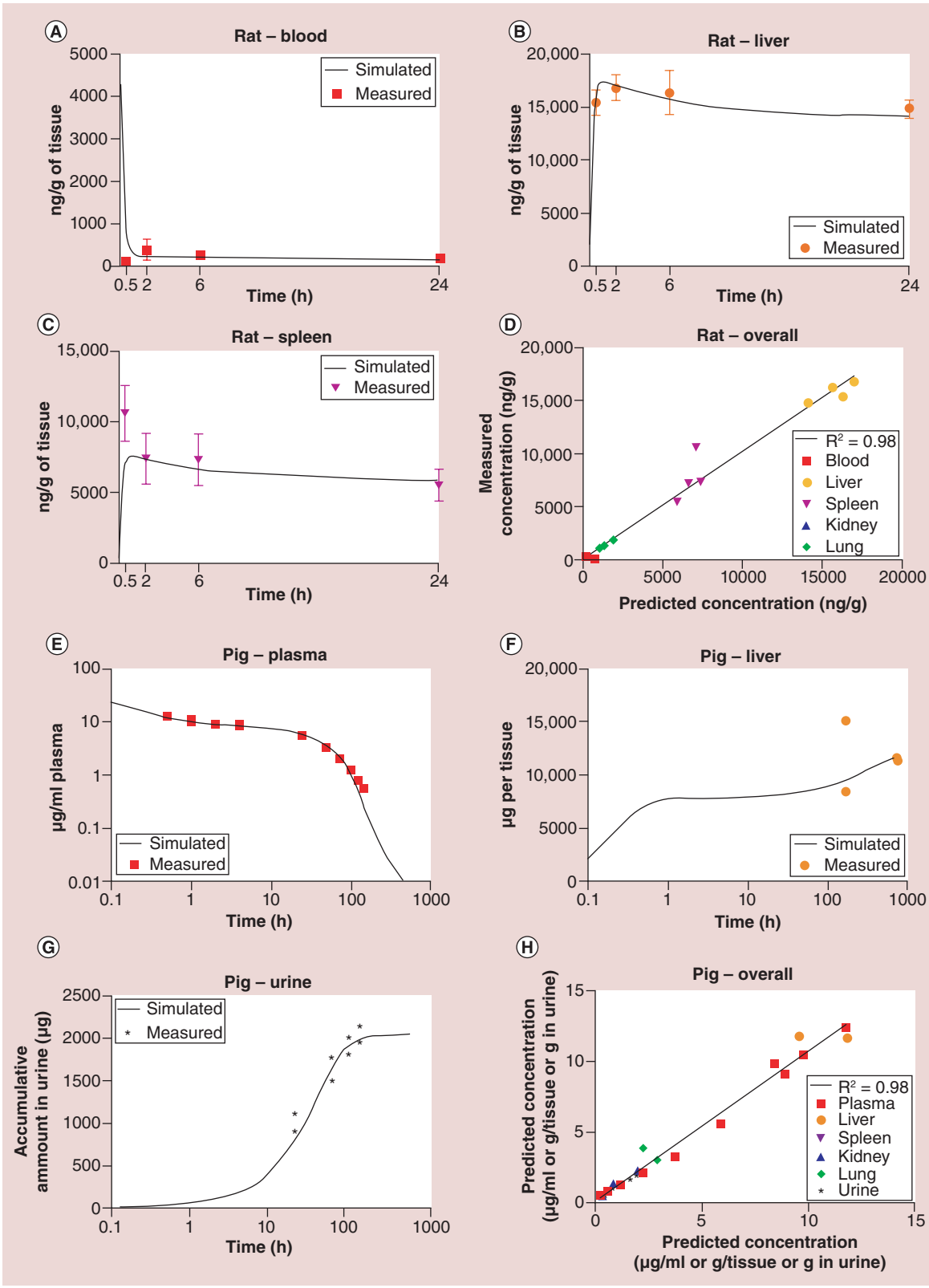

Figure 2. Rat and pig physiologically based pharmacokinetic model calibration. Plots of experimentally determined [25,27] (symbols) versus rat **(A–C)** and pig **(E–G)** model-predicted (lines) concentrations of gold nanoparticles in blood (or plasma), tissues and urine. **(D)** (Rat model) and **(H)** (pig model) represent overall regression analysis results between measured and simulated data. Lines in **(D & H)** represent the regression lines. R^2: Determination coefficient.

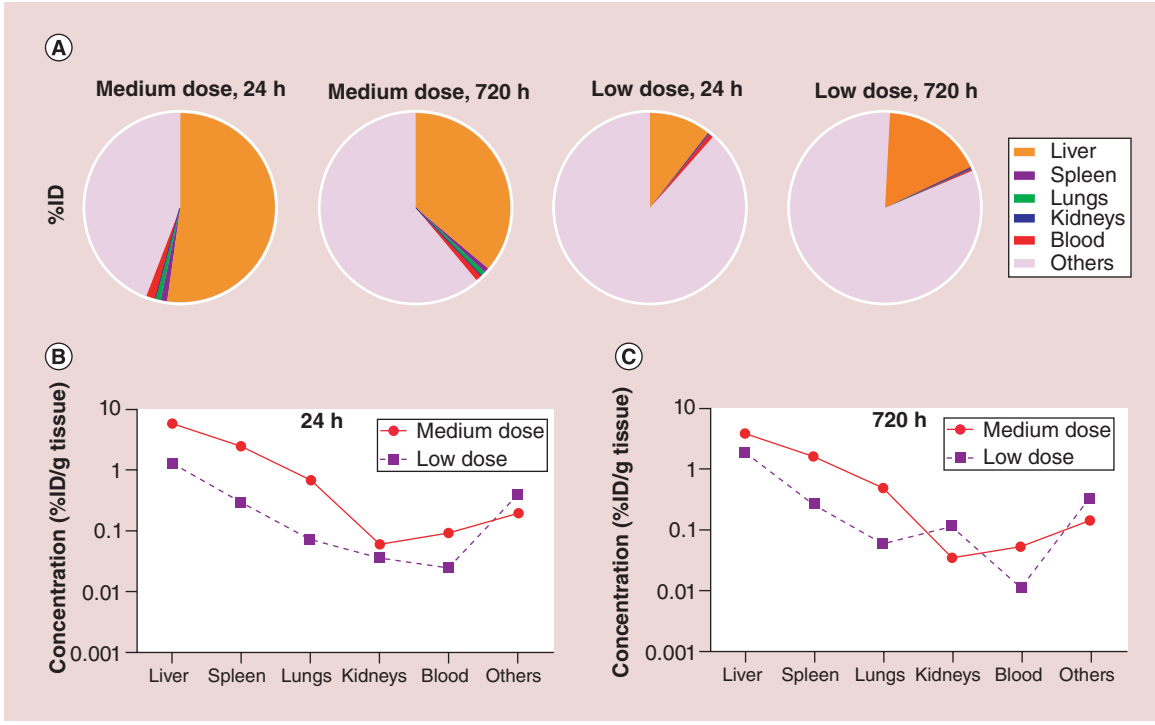

Figure 3. Rat model prediction of dose-dependent pharmacokinetics of gold nanoparticles. Simulation results of absolute (**[A]**; %ID) and relative (**[B & C]**; %ID/g tissue) percentage injected doses in blood and representative tissues of rats at 24 and 720 h after intravenous injection with 0.01 mg/kg gold nanoparticles. 'Medium dose' and 'low dose' indicate results predicted by using the medium-dose and low-dose rat models, respectively.

dose-dependent pharmacokinetics, especially when extrapolating across species.

Evaluation of model extrapolation from mice, rats or pigs to humans

To assess which of the studied PBPK models can be extrapolated successfully to humans, we scaled the rodent and porcine models to humans by using the human-specific physiological parameter (e.g., blood flow) and keeping the endocytic parameters the same as those in each respective animal model (Figure 1). The derived human models were employed to simulate blood concentrations of AuNP-based nanomedicine (CYT-6091) in humans [39]. As shown in Figures 1 and 4, the human models derived from the mouse model, medium-dose rat model or original pig model failed to capture the blood kinetic profiles ($R^2 < 0.87$), but the human models derived from the low-dose rat model and the revised pig model properly simulated the measured blood levels of AuNP, with the R^2 values being 0.9427 and 0.9368, respectively. Based on the R^2 value, the human model derived from the low-dose rat model was selected as the optimal human model for subsequent analyses.

Discussion

The pharmacokinetics and safety of NP are routinely evaluated in laboratory animals prior to applications in humans. Thus, it is crucial to understand interspecies difference in NP pharmacokinetics before we confidently use data generated in laboratory animal species to make inferences in humans. The present study successfully established a comprehensive computational framework that properly simulated tissue distribution of AuNP across several species. One of the most important findings is that rats and pigs appear to be more appropriate model species than mice in animal-to-human extrapolation of NP pharmacokinetics and the dose and age should be considered for this extrapolation. This computational comparative analysis of NP pharmacokinetics is novel in the field of nanotechnology.

The key finding that rats and pigs seem to be more suitable models than mice may be a function of different surface coatings, sizes, doses, ages and/or species/strain/breed among the different studies used in model calibration and evaluation [23,25-27,39]. The explanation of surface coatings is unlikely because the mouse and human studies both used PEG-coated AuNP [23,39], a coating that minimizes species differences in protein corona effects [5-6,9] that would be expected for NP of different coatings that facilitate protein adsorption. In addition, the particle size difference is less likely to be of concern because the sizes used in the mouse, rat, pig and human studies were

quite close (13–27 nm) [23,25-27,39]. The fact that the doses (0.001286–0.01726 mg/kg) used in the human study [39] are close to the low-dose rat study [26], but far lower than the medium-dose rat study [27], suggests that dose-dependent disposition is the likely factor. A second possible reason is the difference in the relative density of phagocytic cells in major organs between juvenile pigs and adult humans [40,41]. Therefore, we revised the original pig-model-derived human model based on the relative density of Kupffer cells in juvenile pigs and adult humans [40,41]. Simulation results from the revised pig-model-derived human model were well correlated with the observed human data (Figure 4). These results suggest that extrapolations of NP pharmacokinetics from rats or pigs to humans are plausible provided that the species-specific model parameters are adjusted appropriately. The fact that the present models converged does imply that it is possible to conduct interspecies extrapolations for such covered particles. However, whether this conclusion applies to AuNP with other surface functionalizations remains to be investigated.

The reason that rats and pigs may be more suitable models than mice in extrapolating NP pharmacokinetics to humans is multifaceted. Anatomically, the mouse and pig spleen capillaries are nonsinusoidal with predominant blood flow through the open-circulation route where NP filtration is mainly regulated by barrier cells; but the spleen capillaries in rats and humans are both sinusoidal, where the large part of blood flows through open-circulation routes with NP filtration at interendothelial cell slits [46]. The liver capillaries of mice, rats, pigs and humans are all sinusoidal with open fenestrae, but the average number of fenestrae per square micrometer in mice is lower than that of rats and humans (this number is 14, 20 and 20 in mice, rats and humans, respectively, but it is not available for pigs) [47]. Blood flows to some organs (e.g., liver, skin) are age- and species-dependent [48,49]. Age difference in selected studies may thus be an important factor in our observed results. Immunologically, there are species differences in the plasma membrane receptor expression and functionality of macrophages [50] that may play a significant role in the NP opsonization, endocytosis and clearance. Physiologically, there are several parameters (e.g., liver weight fraction of body weight) that greatly affect NP pharmacokinetics, and rats and pigs are closer to humans than mice in these parameters [23]. The fact that the majority of NP-based drug formulations that are seemingly effective to decrease tumor sizes in mice, but are not effective in humans, further supports this supposition [51]. Overall, our finding is novel and it further questions the conventional wisdom of nanotoxicology evaluation solely using the mouse model. Nevertheless, at this stage, definitive conclusion cannot be made because there are differences in the AuNP used in different studies for model calibration, and strain differences within rodents could also play a role. While available data are very limited, the types of physiological and pharmacokinetic processes included in this model need to be taken into account whenever results seen in a rodent model are attempted to be extrapolated to humans. Additional comparative pharmacokinetic studies with rodents and pigs at similar ages using the same type of NP are needed to confirm these findings.

The above-mentioned fundamental anatomical, immunological and physiological differences between species are difficult to compensate for in a mathematical model because there is lack of sufficiently granular *in vivo* pharmacokinetic data in order to separate out the different mechanisms. Nevertheless, a computational framework built on PBPK modeling provides the most promising approach to integrate various mechanistic factors into whole body cross-species predictive models. It has been demonstrated that PEGylation of AuNP is unstable *in vivo* due to the degradation of the polymer shell by proteolytic enzymes in the liver [52]. The effect of the unstability of PEGylation on AuNP pharmacokinetics is not mathematically evaluated due to the lack of time-intensive pharmacokinetic data for the same AuNP with and without PEGylation in more than two species. Another issue is that particle physicochemical properties, such as the state of agglomeration and surface charge, are not mathematically introduced into the model because there are not adequate data to simulate these factors. Once the aforementioned data are available, this present framework provides a computational platform to incorporate various factors to decipher the pharmacokinetic characteristics of NP.

To demonstrate model application in exposure and risk assessment, a comprehensive literature review on the AuNP toxicity was conducted (Supplementary Table 4). In order to provide a conservative risk assessment, the lowest reported toxic concentrations of AuNP in rats [26], human tissue [43] and blood cells [44] were selected. The associated human equivalent doses were calculated by using the optimal human model (Figure 5). The congruence of these results suggests that our model provides a framework to integrate *in vitro* and *in vivo* toxicity studies to inform NP exposure and risk assessment. These results are informative for the design of human clinical trials.

Of note, this framework can be used to correlate NP *in vitro* cellular uptake to *in vivo* pharmacokinet-

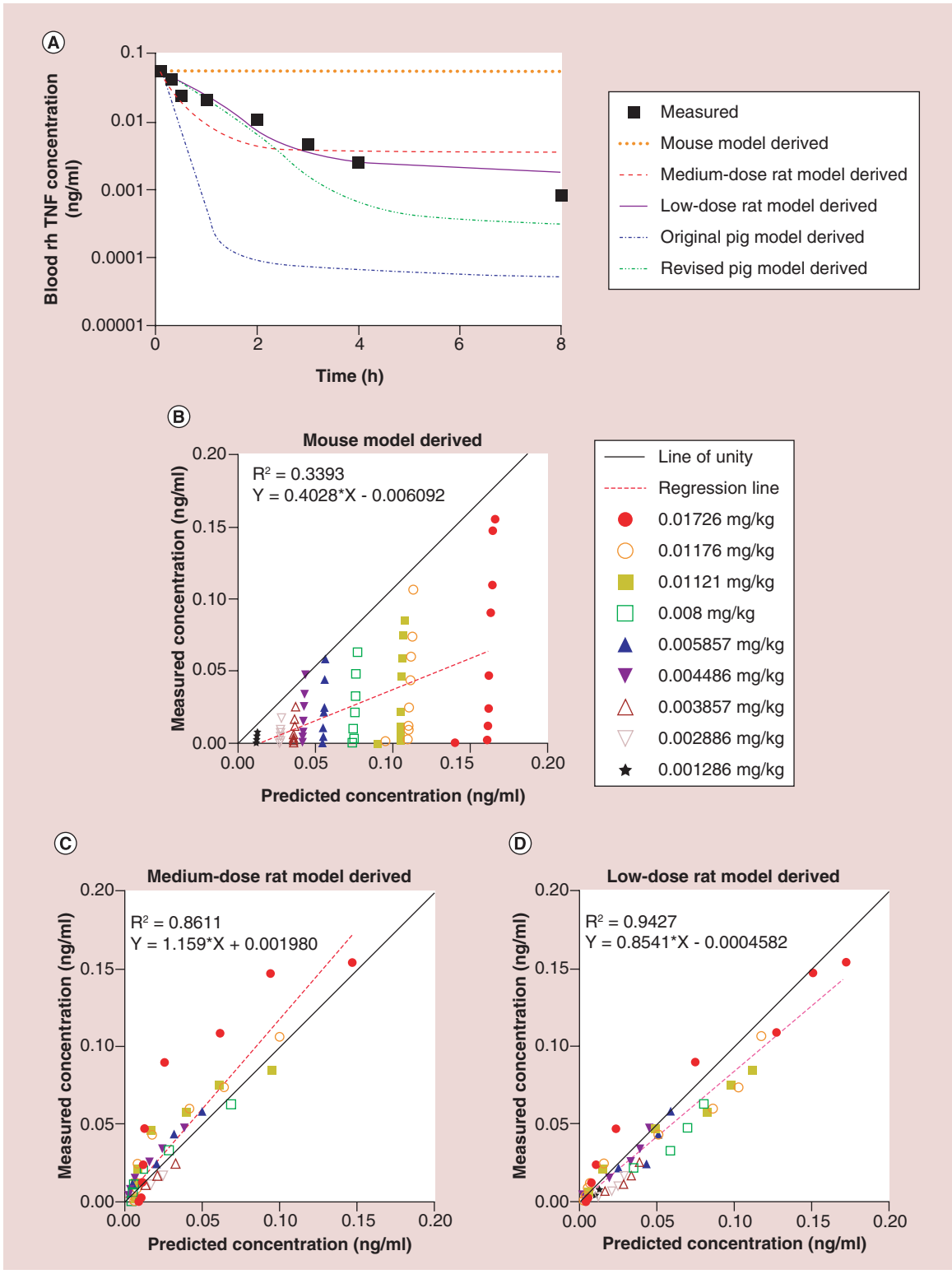

Figure 4. Physiologically based pharmacokinetic model species extrapolation (for [A–D], please see above; for [E & F], please see facing page). (A) Comparisons of experimental [39] (symbols) versus predicted (lines) blood concentrations of gold nanoparticles after intravenous injection (0.005857 mg/kg) using human models derived from different animal models. Animal-to-human extrapolation was conducted by changing the physiological parameters to be human-specific and keeping the endocytic and other nanoparticle-specific parameters the same as in the original animal models.

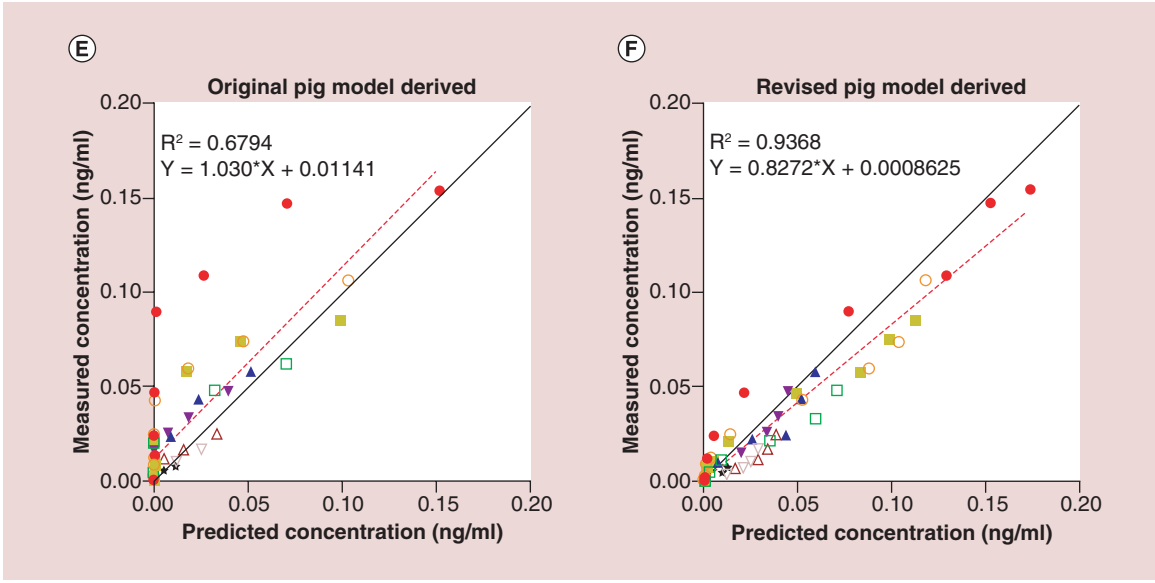

Figure 4. Physiologically based pharmacokinetic model species extrapolation (cont.). (B–F) Represent regression analysis results between experimental [39] and predicted values for different models. Different symbols indicate results from different dose groups. The black straight lines represent perfect agreement between experimental and predicted data. The red dashed lines represent regression lines. Regression equations are given in each panel. R^2: Determination coefficient.

ics, thus raising a possibility of developing NP PBPK models using alternative approaches. To be more specific, for all NP-specific parameters among different models in this framework, the distribution and permeability parameters are the same across models, but the endocytic parameters are model-specific. Thus, NP PBPK models may be created based on the present model framework and using species- and dose-specific endocytic parameters measured *in vitro*. Currently, there are a number of *in vitro* studies investigating cellular uptake of various NP, including AuNP, but most of these studies focus on uptake mechanisms and NP's fate after cellular internalization [6]. The experimental designs of available studies make it difficult to conduct IVIVE. To address this significant data gap, the present model was designed to include *in vitro* cellular uptake kinetic parameters. The following suggestions need to be considered in designing future cellular uptake studies. First, cell models should include the type of cells in which NP mainly accumulate *in vivo*, such as Kupffer cells and spleen/lung macrophages which are the rate-limiting factors in systemic NP biodistribution. Wherever possible the primary cell type should be used rather than an immortalize cell line. A time-dependent study should also be conducted to identify the optimal incubation time when the uptake rate is at the maximum prior to a concentration-dependent study to determine the uptake kinetics. Data should be expressed in the unit of 'ng/h/cell,' so that the data can be converted to 'µg/h' for a particular tissue. Next, an appropriate mathematical equation (e.g., the Hill function) should be used to fit the concentration-dependent uptake kinetic data, in which related kinetic parameters can be calculated and incorporated into the present PBPK model. In addition to the *in vitro* cellular uptake studies, *in vitro* toxicity studies using the same human cells, *in vivo* toxicity studies with rats at <0.01 mg/kg doses and mechanistic pharmacokinetic modeling studies taking into account species differences in physiology and anatomy are warranted. Finally, this model based on PEG-coated AuNP does not take into account species differences in protein corona formation which could further impact PBPK model structure and interspecies extrapolations [9]. An approach to deal with timescale differences in protein corona formation in non-PEGylated NP has been addressed [9]. All of these proposed suggestions should be incorporated into the present computational framework to improve the risk assessment of AuNP.

Conclusion & future perspective

Our laboratory successfully developed an integrative comprehensive comparative PBPK model that predicts the pharmacokinetics of AuNP across multiple species and provides a foundation to incorporate *in vitro* and *in vivo* toxicity data for quantitative risk assessment. Simulation results provide systematic guidance for the design of future studies. This comprehensive comparative PBPK modeling approach could be extrapolated to other types of nanomaterials and thus opens a quan-

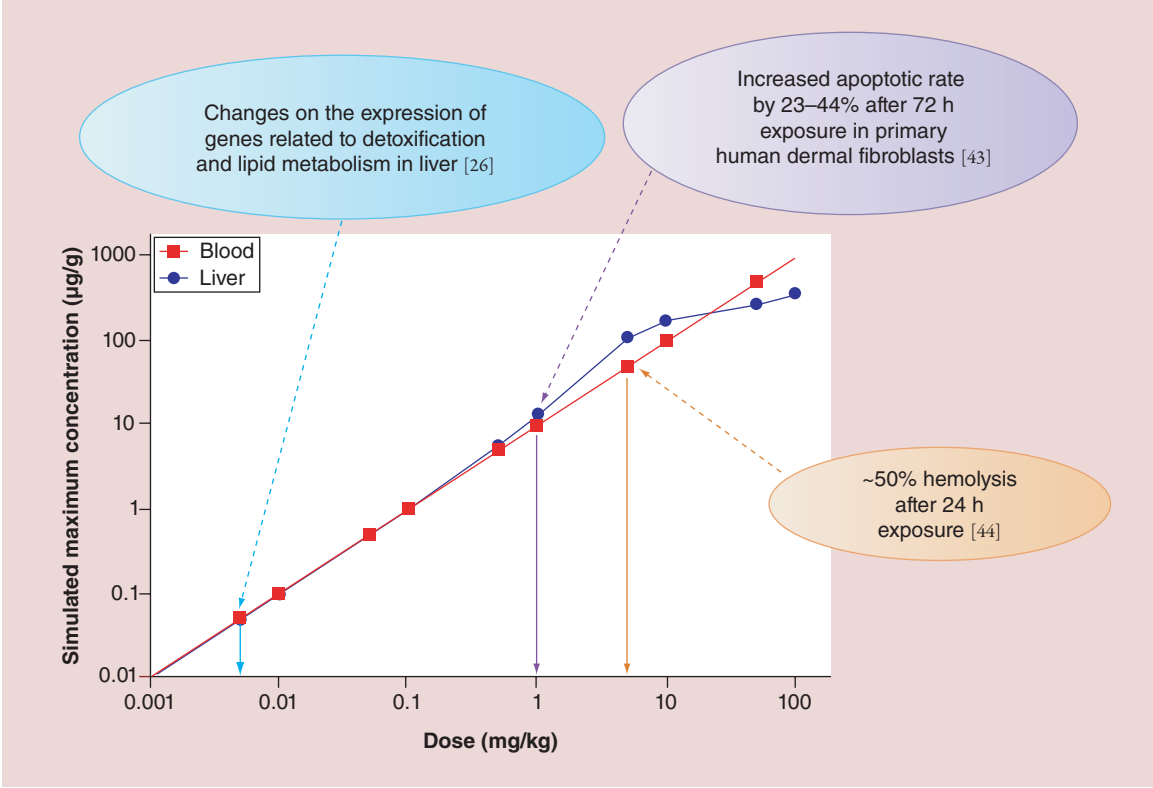

Figure 5. *In vitro* to *in vivo* extrapolation and species extrapolation of doses and toxicity of gold nanoparticles. Blue and red lines represent model-predicted maximum concentrations of gold nanoparticles in the liver and blood, respectively, of humans after intravenous injection (0.001–100 mg/kg). The dashed arrows point to concentrations of gold nanoparticles where *in vitro* cytotoxicity (13 μg/ml) or hemolysis (50 μg/ml) was observed in primary human dermal fibroblasts [43] and blood cells [44] or where liver toxicity (0.01 mg/kg) was observed in rats [26]. Reference citations are given in square brackets. The solid arrows point to the model-predicted human equivalent dose (HED) associated with the reported *in vitro* cytotoxicity (HED = 1 mg/kg), hemolysis (HED = 5 mg/kg) and *in vivo* toxicity (HED = 0.005 mg/kg).

titative research avenue toward predictive nanotoxicity assessment, safety evaluation of NP-based drug formulations and NP interspecies pharmacokinetic extrapolation.

Supplementary data

To view the supplementary data that accompany this paper, please visit the journal website at: www.futuremedicine.com/doi/full/10.2217/NNM.15.177

Executive summary

- Interspecies and *in vitro* to *in vivo* extrapolations of pharmacokinetic and toxicology data are crucial for successful translation from laboratory studies to humans and for proper risk assessment of nanomaterials.
- We developed a comprehensive computational framework built on physiologically based pharmacokinetic modeling that successfully simulated tissue distribution of gold nanoparticles across a wide dose range and several species, including mice, rats and pigs.
- Animal-to-human extrapolation of nanomaterial pharmacokinetics was performed from mice, rats and pigs, respectively, to humans.
- Rats and pigs seem to be more appropriate models than mice in species extrapolation of nanomaterial pharmacokinetics to humans and that the dose and age should be considered.
- Our results provide a scientific basis for researchers to select the most appropriate animal model and dosing paradigm for conducting future nanomaterial studies to increase the research relevance to humans.
- Our model can be used to incorporate *in vitro* and *in vivo* cellular uptake and toxicity data to improve risk assessment of nanomaterials.
- This simulation approach may be applied to other types of nanomaterials and provides guidance to the design of future pharmacokinetic, toxicological and translational studies of nanomaterials.

Disclaimer

The sponsors had no role in study design, data collection, model development, data analysis or manuscript preparation.

Financial & competing interests disclosure

This study was supported by the Kansas Bioscience Authority funds to the Institute of Computational Comparative Medicine (ICCM) and the Nanotechnology Innovation Center of Kansas State (NICKS) at Kansas State University. The authors have no other relevant affiliations or financial involvement with any organization or entity with a financial interest in or financial conflict with the subject matter or materials discussed in the manuscript apart from those disclosed.

No writing assistance was utilized in the production of this manuscript.

References

Papers of special note have been highlighted as:
• of interest; •• of considerable interest

1 Yamashita K, Yoshioka Y, Higashisaka K *et al.* Silica and titanium dioxide nanoparticles cause pregnancy complications in mice. *Nat. Nanotechnol.* 6(5), 321–328 (2011).

2 Khlebtsov N, Dykman L. Biodistribution and toxicity of engineered gold nanoparticles: a review of *in vitro* and *in vivo* studies. *Chem. Soc. Rev.* 40(3), 1647–1671 (2011).

3 Oberdörster G, Stone V, Donaldson K. Toxicology of nanoparticles: a historical perspective. *Nanotoxicology* 1(1), 2–25 (2007).

4 Nel A, Xia T, Madler L, Li N. Toxic potential of materials at the nanolevel. *Science* 311(5761), 622–627 (2006).

5 Lin Z, Monteiro-Riviere NA, Riviere JE. Pharmacokinetics of metallic nanoparticles. *Wiley Interdiscip. Rev. Nanomed. Nanobiotechnol.* 7(2), 189–217 (2015).

6 Dykman LA, Khlebtsov NG. Uptake of engineered gold nanoparticles into mammalian cells. *Chem. Rev.* 114(2), 1258–1288 (2014).

7 Landsiedel R, Fabian E, Ma-Hock L *et al.* Toxico-/biokinetics of nanomaterials. *Arch. Toxicol.* 86(7), 1021–1060 (2012).

8 Godwin H, Nameth C, Avery D *et al.* Nanomaterial categorization for assessing risk potential to facilitate regulatory decision-making. *ACS Nano* 9(4), 3409–3417 (2015).

9 Sahneh FD, Scoglio CM, Monteiro-Riviere NA, Riviere JE. Predicting the impact of biocorona formation kinetics on interspecies extrapolations of nanoparticle biodistribution modeling. *Nanomedicine (Lond.)* 10(1), 25–33 (2015).

•• **Describes the impact of biocorona formation kinetics on the pharmacokinetics of nanomaterials across species.**

10 Riviere JE. Of mice, men and nanoparticle biocoronas: are *in vitro* to *in vivo* correlations and interspecies extrapolations realistic? *Nanomedicine (Lond.)* 8(9), 1357–1359 (2013).

11 Li M, Al-Jamal KT, Kostarelos K, Reineke J. Physiologically based pharmacokinetic modeling of nanoparticles. *ACS Nano* 4(11), 6303–6317 (2010).

•• **The first review article on the applications of physiologically based pharmacokinetic modeling in nanomaterial pharmacokinetics and toxicology studies.**

12 Teeguarden JG, Hinderliter PM, Orr G, Thrall BD, Pounds JG. Particokinetics *in vitro*: dosimetry considerations for *in vitro* nanoparticle toxicity assessments. *Toxicol. Sci.* 95(2), 300–312 (2007).

•• **Develops and applies the principles of nanomaterial dosimetry *in vitro* and outlines an approach for simulating nanoparticle particokinetics in cell culture systems.**

13 Xia XR, Monteiro-Riviere NA, Riviere JE. An index for characterization of nanomaterials in biological systems. *Nat. Nanotechnol.* 5(9), 671–675 (2010).

14 Meng H, Xia T, George S, Nel AE. A predictive toxicological paradigm for the safety assessment of nanomaterials. *ACS Nano* 3(7), 1620–1627 (2009).

• **Proposes a predictive toxicological approach for the assessment of nanomaterial hazards.**

15 Cohen JM, Teeguarden JG, Demokritou P. An integrated approach for the *in vitro* dosimetry of engineered nanomaterials. *Part. Fibre Toxicol.* 11, 20 (2014).

16 Liu R, Rallo R, Weissleder R, Tassa C, Shaw S, Cohen Y. Nano-SAR development for bioactivity of nanoparticles with considerations of decision boundaries. *Small* 9(9–10), 1842–1852 (2013).

17 Puzyn T, Rasulev B, Gajewicz A *et al.* Using nano-QSAR to predict the cytotoxicity of metal oxide nanoparticles. *Nat. Nanotechnol.* 6(3), 175–178 (2011).

18 Speck-Planche A, Kleandrova VV, Luan F, Cordeiro MN. Computational modeling in nanomedicine: prediction of multiple antibacterial profiles of nanoparticles using a quantitative structure-activity relationship perturbation model. *Nanomedicine (Lond.)* 10(2), 193–204 (2015).

19 Kleandrova VV, Luan F, Gonzalez-Diaz H, Ruso JM, Speck-Planche A, Cordeiro MN. Computational tool for risk assessment of nanomaterials: novel QSTR-perturbation model for simultaneous prediction of ecotoxicity and cytotoxicity of uncoated and coated nanoparticles under multiple experimental conditions. *Environ. Sci. Technol.* 48(24), 14686–14694 (2014).

20 Lee HA, Leavens TL, Mason SE, Monteiro-Riviere NA, Riviere JE. Comparison of quantum dot biodistribution with a blood-flow-limited physiologically based pharmacokinetic model. *Nano Lett.* 9(2), 794–799 (2009).

21 Li D, Johanson G, Emond C, Carlander U, Philbert M, Jolliet O. Physiologically based pharmacokinetic modeling of polyethylene glycol-coated polyacrylamide nanoparticles in rats. *Nanotoxicology* 8, 128–137 (2014).

22 Bachler G, Von Goetz N, Hungerbuhler K. Using physiologically based pharmacokinetic (PBPK) modeling for dietary risk assessment of titanium dioxide (TiO) nanoparticles. *Nanotoxicology* 9(3), 373–380 (2015).

23 Lin Z, Monteiro-Riviere NA, Riviere JE. A physiologically based pharmacokinetic model for polyethylene glycol-coated gold nanoparticles of different sizes in adult mice. *Nanotoxicology* doi:10.3109/17435390.2015.1027314 (2015) (Epub ahead of print).

24 Sasidharan A, Monteiro-Riviere NA. Biomedical applications of gold nanomaterials: opportunities and challenges. *Wiley Interdiscip. Rev. Nanomed. Nanobiotechnol.* 7(6), 779–796 (2015).

25 Fent GM, Casteel SW, Kim DY *et al.* Biodistribution of maltose and gum arabic hybrid gold nanoparticles after intravenous injection in juvenile swine. *Nanomedicine* 5(2), 128–135 (2009).

26 Balasubramanian SK, Jittiwat J, Manikandan J, Ong CN, Yu LE, Ong WY. Biodistribution of gold nanoparticles and gene expression changes in the liver and spleen after intravenous administration in rats. *Biomaterials* 31(8), 2034–2042 (2010).

27 Morais T, Soares ME, Duarte JA *et al.* Effect of surface coating on the biodistribution profile of gold nanoparticles in the rat. *Eur. J. Pharm. Biopharm.* 80(1), 185–193 (2012).

28 Pharmacokinetic model database at the Institute of Computational Comparative Medicine at Kansas State University. http://iccm.k-state.edu/

29 Lin Z, Li M, Gehring R, Riviere JE. Development and application of a multiroute physiologically based pharmacokinetic model for oxytetracycline in dogs and humans. *J. Pharm. Sci.* 104(1), 233–243 (2015).

30 Lin Z, Fisher JW, Wang R, Ross MK, Filipov NM. Estimation of placental and lactational transfer and tissue distribution of atrazine and its main metabolites in rodent dams, fetuses, and neonates with physiologically based pharmacokinetic modeling. *Toxicol. Appl. Pharmacol.* 273(1), 140–158 (2013).

31 Crowell SR, Henderson WM, Kenneke JF, Fisher JW. Development and application of a physiologically based pharmacokinetic model for triadimefon and its metabolite triadimenol in rats and humans. *Toxicol. Lett.* 205(2), 154–162 (2011).

32 Upton RN. Organ weights and blood flows of sheep and pig for physiological pharmacokinetic modelling. *J. Pharmacol. Toxicol. Methods* 58(3), 198–205 (2008).

33 Buur JL, Baynes RE, Craigmill AL, Riviere JE. Development of a physiologic-based pharmacokinetic model for estimating sulfamethazine concentrations in swine and application to prediction of violative residues in edible tissues. *Am. J. Vet. Res.* 66(10), 1686–1693 (2005).

34 Brown RP, Delp MD, Lindstedt SL, Rhomberg LR, Beliles RP. Physiological parameter values for physiologically based pharmacokinetic models. *Toxicol. Ind. Health* 13(4), 407–484 (1997).

35 Davies B, Morris T. Physiological parameters in laboratory animals and humans. *Pharm. Res.* 10(7), 1093–1095 (1993).

36 Kattumuri V, Katti K, Bhaskaran S *et al.* Gum arabic as a phytochemical construct for the stabilization of gold nanoparticles: *in vivo* pharmacokinetics and x-ray-contrast-imaging studies. *Small* 3(2), 333–341 (2007).

37 Fraga S, Brandao A, Soares ME *et al.* Short- and long-term distribution and toxicity of gold nanoparticles in the rat after a single-dose intravenous administration. *Nanomedicine* 10(8), 1757–1766 (2014).

38 International Programme on Chemical Safety Harmonization Project Document No. 9. Characterization and application of physiologically based pharmacokinetic models in risk assessment. World Health Organization, Geneva, Switzerland, 1–91 (2010).

39 Libutti SK, Paciotti GF, Byrnes AA *et al.* Phase I and pharmacokinetic studies of CYT-6091, a novel PEGylated colloidal gold-rhTNF nanomedicine. *Clin. Cancer Res.* 16(24), 6139–6149 (2010).

- **Reports the plasma pharmacokinetics of a gold nanoparticle-based nanomedicine in human cancer patients.**

40 Akunda JK, Ahrens FA, Kramer TT. Evaluation of phagocytosis, bactericidal activity, and production of superoxide anion, nitric oxide, and tumor necrosis factor-alpha in Kupffer cells of neonatal pigs. *Am. J. Vet. Res.* 62(7), 1040–1045 (2001).

41 Alabraba EB, Curbishley SM, Lai WK, Wigmore SJ, Adams DH, Afford SC. A new approach to isolation and culture of human Kupffer cells. *J. Immunol. Methods* 326(1–2), 139–144 (2007).

42 Moghimi SM, Hunter AC, Andresen TL. Factors controlling nanoparticle pharmacokinetics: an integrated analysis and perspective. *Annu. Rev. Pharmacol. Toxicol.* 52, 481–503 (2012).

43 Mironava T, Hadjiargyrou M, Simon M, Jurukovski V, Rafailovich MH. Gold nanoparticles cellular toxicity and recovery: effect of size, concentration and exposure time. *Nanotoxicology* 4(1), 120–137 (2010).

44 Love SA, Thompson JW, Haynes CL. Development of screening assays for nanoparticle toxicity assessment in human blood: preliminary studies with charged Au nanoparticles. *Nanomedicine (Lond.)* 7(9), 1355–1364 (2012).

45 Martin SA, Mclanahan ED, Bushnell PJ, Hunter ES, 3rd, El-Masri H. Species extrapolation of life-stage physiologically-based pharmacokinetic (PBPK) models to investigate the developmental toxicology of ethanol using *in vitro* to *in vivo* (IVIVE) methods. *Toxicol. Sci.* 143(2), 512–535 (2015).

46 Cesta MF. Normal structure, function, and histology of the spleen. *Toxicol. Pathol.* 34(5), 455–465 (2006).

47 Braet F, Wisse E. Structural and functional aspects of liver sinusoidal endothelial cell fenestrae: a review. *Comp. Hepatol.* 1(1), 1 (2002).

48 Monteiro-Riviere NA, Banks YB, Birnbaum LS. Laser Doppler measurements of cutaneous blood flow in ageing mice and rats. *Toxicol. Lett.* 57(3), 329–338 (1991).

49 Mclean AJ, Le Couteur DG. Aging biology and geriatric clinical pharmacology. *Pharmacol. Rev.* 56(2), 163–184 (2004).

50 Gordon S, Taylor PR. Monocyte and macrophage heterogeneity. *Nat. Rev. Immunol.* 5(12), 953–964 (2005).

51 Park K. Facing the truth about nanotechnology in drug delivery. *ACS Nano* 7(9), 7442–7447 (2013).

52 Kreyling WG, Abdelmonem AM, Ali Z *et al. In vivo* integrity of polymer-coated gold nanoparticles. *Nat. Nanotechnol.* 10(7), 619–623 (2015).

• **Demonstrates that gold nanoparticles coated with polymer shells can change their physicochemical properties *in vivo* due to degradation of the polymer shell by proteolytic enzymes in the liver.**